Cell Metabolism
Article

APPL1 Potentiates Insulin-Mediated Inhibition of Hepatic Glucose Production and Alleviates Diabetes via Akt Activation in Mice

Kenneth K.Y. Cheng,[1,2] Miguel A. Iglesias,[3] Karen S.L. Lam,[1,2] Yu Wang,[2,4] Gary Sweeney,[5] Weidong Zhu,[1,2] Paul M. Vanhoutte,[2,4] Edward W. Kraegen,[3,*] and Aimin Xu[1,2,4,*]
[1]Department of Medicine
[2]Research Center of Heart, Brain, Hormone and Healthy Aging
The University of Hong Kong, Hong Kong
[3]Garvan Institute of Medical Research and School of Medical Sciences, University of NSW, Sydney, NSW 2010, Australia
[4]Department of Pharmacology, The University of Hong Kong, Hong Kong
[5]Department of Biology, York University, Toronto, ON M3J 1P3, Canada
*Correspondence: e.kraegen@garvan.org.au (E.W.K.), amxu@hkucc.hku.hk (A.X.)
DOI 10.1016/j.cmet.2009.03.013

SUMMARY

Hepatic insulin resistance is the major contributor to fasting hyperglycemia in type 2 diabetes. Here we report that the endosomal adaptor protein APPL1 increases hepatic insulin sensitivity by potentiating insulin-mediated suppression of the gluconeogenic program. Insulin-stimulated activation of Akt and suppression of gluconeogenesis in hepatocytes are enhanced by APPL1 overexpression, but are attenuated by APPL1 knockdown. APPL1 interacts with Akt and blocks the association of Akt with its endogenous inhibitor tribble 3 (TRB3) through direct competition, thereby promoting Akt translocation to the plasma membrane and the endosomes for further activation. In *db/db* diabetic mice, the blockage of the augmented interaction between Akt and TRB3 by hepatic overexpression of APPL1 is accompanied by a marked attenuation of hyperglycemia and insulin resistance. These results suggest that the potentiating effects of APPL1 on insulin-stimulated suppression of hepatic glucose production are attributed to its ability in counteracting the inhibition of Akt activation by TRB3.

INTRODUCTION

The liver is the primary organ responsible for endogenous glucose production, which is tightly controlled by various metabolic and nutritional factors (Accili, 2004). In the fasted state, hepatic glucose production (HGP) is enhanced by glucagon to maintain euglycemia, thus ensuring that glucose-dependent tissues such as the brain have access to an energy supply. When blood glucose levels are elevated after nutrient ingestion, HGP is suppressed by insulin (Barthel and Schmoll, 2003). The inhibitory effect of insulin on HGP is mediated by activation of Akt (also known as protein kinase B). Akt reduces the expression of the key gluconeogenic enzymes phosphoenolpyruvate carboxykinase (*PEPCK*) and glucose 6-phosphatase (*G6Pase*) by suppressing the activity of FOXO1, a member of the forkhead family of transcription factors (Accili, 2004; Nakae et al., 2002). In the absence of insulin, FOXO1 is localized in the nucleus, where it transactivates the two gluconeogenic genes. Upon insulin stimulation, activated Akt phosphorylates FOXO1 at three conserved sites, inducing FOXO1 translocation to the cytoplasm and thereby reducing its transcriptional activity. A key role of the Akt→FOXO1 branch of insulin signaling in suppressing HGP is highlighted by a recent study showing that liver-specific depletion of FOXO1 results in a complete reversal of diabetes in insulin receptor substrate (IRS) 1 and 2 knockout mice (Dong et al., 2008). In addition, activated Akt also inhibits the gluconeogenic program through a phosphorylation-dependent inhibition of the peroxisome proliferator-activated receptor γ coactivator 1 α (PGC-1α) and TORC2, both of which act in concert with FOXO1 in transactivating the gluconeogenic genes (Dentin et al., 2007; Li et al., 2007b; Puigserver et al., 2003).

Hepatic insulin resistance, which leads to excessive HGP, is the major contributor to fasting hyperglycemia in patients with type 2 diabetes mellitus (T2DM) (Biddinger and Kahn, 2006; Magnusson et al., 1992). The central role of excessive HGP in the pathogenesis of T2DM is underscored by the fact that current antidiabetic drugs such as metformin decrease blood glucose levels through inhibiting hepatic gluconeogenesis (Zhou et al., 2001). Therefore, identification of novel molecules involved in regulating the hepatic insulin signaling pathway leading to the inhibition of glucose production might provide potential new targets for novel therapeutic intervention in the treatment of T2DM, a major health burden worldwide.

APPL1, an adaptor protein containing an NH_2-terminal Bin/Amphiphysin/Rvs (BAR) domain, a central pleckstrin homology (PH) domain, and a COOH-terminal phosphotyrosine-binding (PTB) domain (Hosch et al., 2006), was originally identified as an interacting partner of Akt in a yeast two-hybrid assay using Akt2 as a bait (Mitsuuchi et al., 1999). Subsequent studies demonstrate that APPL1 binds to a number of cell-surface receptors (TrkA [Lin et al., 2006; Varsano et al., 2006]; DCC [Liu et al., 2002]), adiponectin (Cheng et al., 2007; Mao et al.,

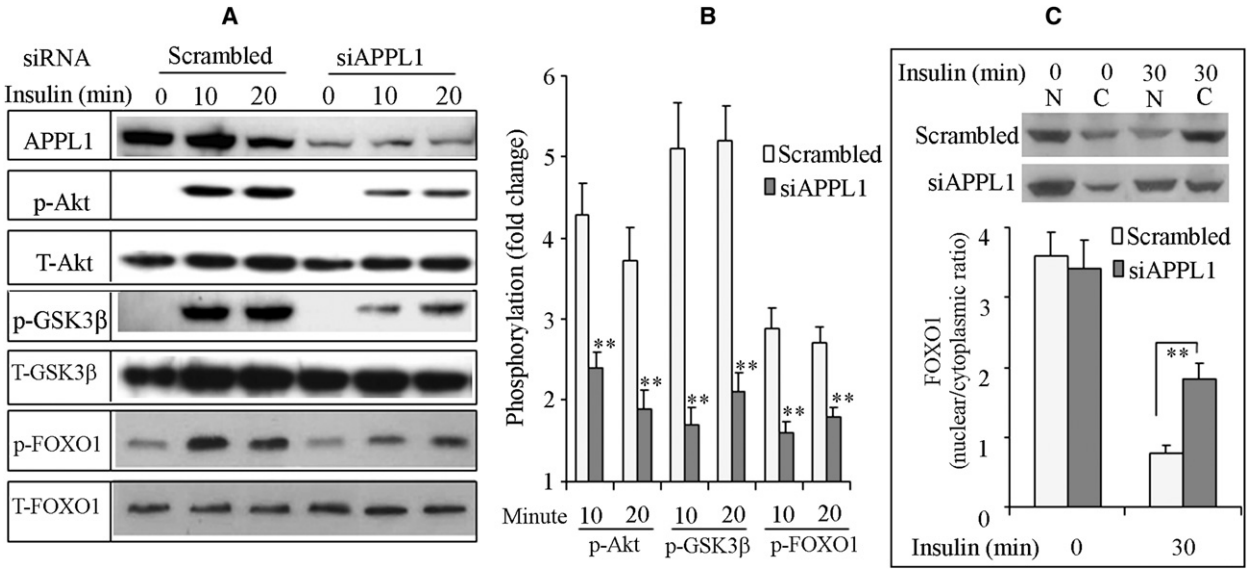

Figure 1. Suppression of APPL1 Expression by siRNA Decreases Insulin-Evoked Activation of the Akt Signaling Pathway and Inhibits the Cytoplasmic Translocation of FOXO1 in Rat Hepatocytes

Cells transduced with adenovirus encoding APPL1 siRNA (siAPPL1) or scrambled control at the concentration of 75 plaque-forming units (p.f.u.)/cell were treated with insulin for various time periods.

(A) Total cell lysates were subjected to immunoblotting analysis using antibodies against total or phospho-Akt (Ser-473), total or phospho-G3K3β (Ser-9), or total or phospho-FOXO1 (Ser-256), as indicated.

(B) The phosphorylation levels of Akt, GSK3β, and FOXO1 were quantified using scanning densitometry, and the results are expressed as fold changes relative to non-insulin-treated control (time = 0 min).

(C) Nuclear (N) and cytoplasmic (C) fractions isolated from cells treated with 10 nM insulin for 0 and 30 min were analyzed by western blot to quantify the subcellular distribution of FOXO1.

Error bars are ±SEM. **$p < 0.01$ ($n = 4–5$).

2006), FSH (Nechamen et al., 2004) and intracellular signaling molecules (small GTPase Rab5; Miaczynska et al., 2004), GIPC (Varsano et al., 2006), and inositol 5-phosphatase (Erdmann et al., 2007), suggesting that APPL1 may act as a common relay to coordinate diverse signaling cascades. Notably, the interaction of APPL1 with adiponectin receptors has recently been shown to be essential in mediating its insulin-sensitizing actions in muscle (Mao et al., 2006) and endothelial cells (Cheng et al., 2007). A more recent study on zebrafish demonstrates that APPL1 not only plays an essential role in Akt activation but also determines Akt substrate specificity (Schenck et al., 2008). In mammalian cells, APPL1 has also been implicated in Akt activation by several extracellular stimuli including androgen (Yang et al., 2003) and NGF-1 (Lin et al., 2006). Furthermore, APPL1 is required for insulin-stimulated translocation of GLUT4 from cytoplasm to plasma membrane and glucose uptake in adipocytes and myotubes (Saito et al., 2007).

Although the aforementioned in vitro findings suggest a potential role of APPL1 as an important player in the insulin-mediated Akt signaling cascade, the physiological functions of APPL1 and the underlying molecular mechanisms have not been explored. In light of the fact that APPL1 is highly expressed in the liver (Mao et al., 2006), we investigated the role of this protein in insulin-mediated inhibition of HGP in both primary hepatocytes and rodent models. In addition, we elucidated the molecular basis whereby APPL1 potentiates insulin-evoked activation of Akt and its downstream targets.

RESULTS

APPL1 Potentiates Insulin-Evoked Akt Signaling in Rat Hepatocytes

To investigate the role of APPL1 in regulating insulin sensitivity in hepatocytes, we employed the adenoviral delivery system for knockdown of this adaptor protein. The APPL1 protein level was decreased by approximately 70% in primary rat hepatocytes infected with adenovirus that encodes a small hairpin RNA (siRNA) specific to the *APPL1* gene, compared with the cells infected with adenovirus encoding a scrambled control (Figure 1A). Knockdown of APPL1 expression attenuated insulin-stimulated phosphorylation of Akt at Ser-473, and consequently reduced the phosphorylation of FOXO1 and glycogen synthase kinase 3β (GSK-3β) (Figures 1A and 1B). Subcellular fractionation analysis showed that insulin stimulation prompted the translocation of FOXO1 from the nucleus to the cytoplasm, whereas this effect of insulin was attenuated in cells with a reduced APPL1 expression (Figure 1C).

To further confirm the above findings, we also examined the effect of APPL1 overexpression in mediating the hepatic actions of insulin (see Figure S1 available online). Infection of rat hepatocytes with recombinant adenovirus encoding full-length human APPL1 for 48 hr led to an approximately 2.5-fold increase in APPL1 protein levels compared to that infected with adenovirus encoding luciferase control. Overexpression of APPL1 markedly increased the magnitude of insulin-evoked phosphorylation of Akt and its two downstream targets (FOXO1 and GSK-3β),

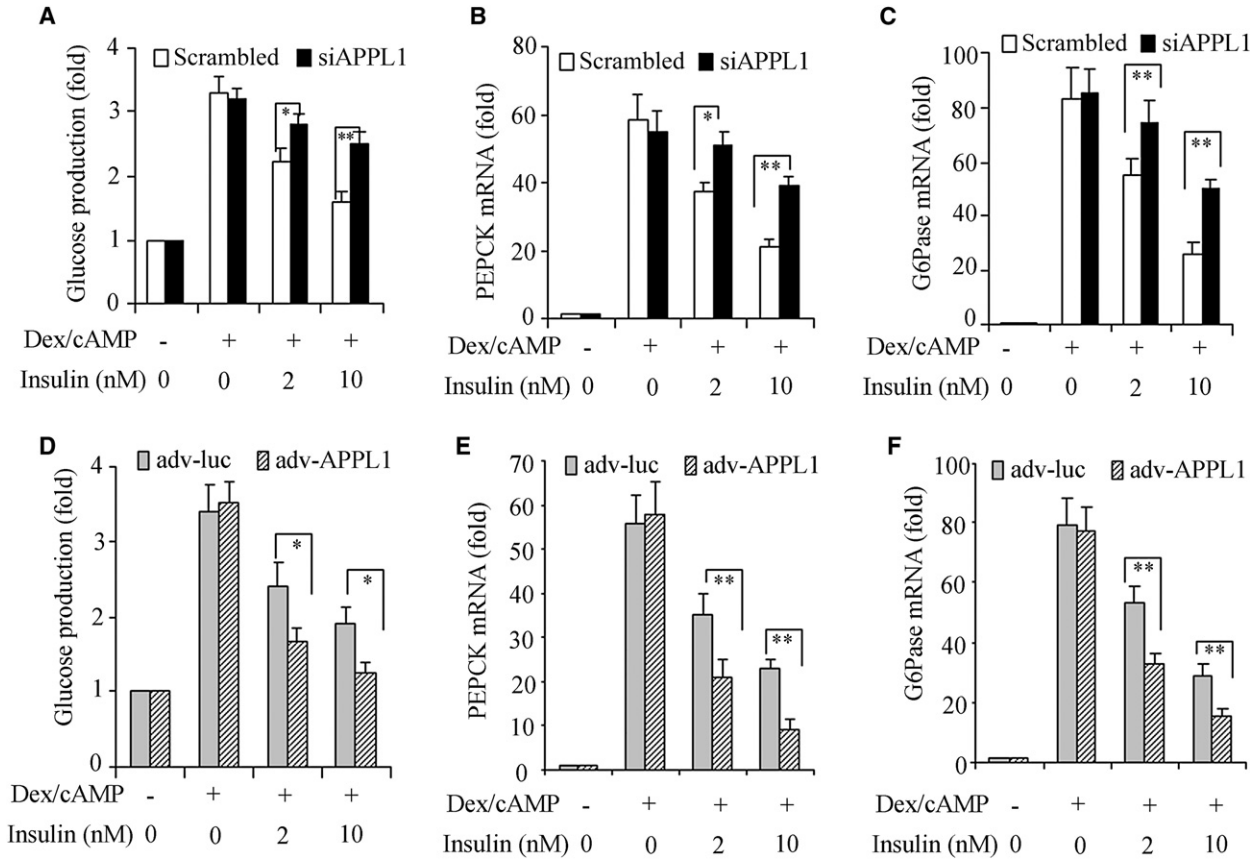

Figure 2. The Suppressive Effects of Insulin on Glucose Production and Gluconeogenic Gene Expression Are Altered by APPL1 Knockdown or Overexpression in Rat Hepatocytes

(A–F) Cells were transduced with adenovirus encoding APPL1-specific siRNA (siAPPL1) or scrambled control (A–C), or with adenovirus encoding APPL1 (adv-APPL1) or luciferase (adv-luc) control (D–F) at the concentration of 75 p.f.u./cell for 48 hr. The effects of insulin on cAMP/Dex-induced glucose production were analyzed as described in Experimental Procedures. The mRNA expression of *PEPCK* and *G6Pase* was quantified by real-time PCR and normalized against 18S RNA.

Error bars are ±SEM. *$p < 0.05$; **$p < 0.01$ ($n = 4–6$).

although the phosphorylation of these proteins under the basal condition were little affected.

APPL1 Enhances Insulin-Mediated Suppression of Hepatic Glucose Production

Treatment of primary hepatocytes with N^6,2′-*O*-dibutyryladenosine 3′,5′-cyclic monophosphate sodium salt (cAMP; 100 μM) and dexamethasone (Dex; 500 nM) resulted in a 3.1-fold increase in glucose production (Figure 2A). Knockdown of APPL1 expression did not affect glucose production under the basal condition or under the stimulation with cAMP/Dex, but markedly attenuated the suppressive effects of insulin on hepatic glucose production. Insulin at the concentrations of 2 and 10 nM inhibited cAMP/Dex-induced glucose production by 33% ± 2% and 58% ± 5%, respectively, in cells infected with a scrambled control, compared to 14% ± 1% and 31% ± 4% reductions in cells infected with APPL1-specific siRNA ($n = 6$, $p < 0.05$ for both comparisons). In addition, siRNA-mediated reduction of APPL1 expression attenuated the suppressive effects of insulin on cAMP/Dex-induced expression of *PEPCK* and *G6Pase*, the two key enzymes involved in gluconeogenesis (Figures 2B and 2C). Conversely, overexpression of APPL1 enhanced the effect of insulin on inhibiting hepatic glucose production and on suppressing the expression of the two gluconeogenic genes (*PEPCK* and *G6Pase*) induced by cAMP/dexamethasone (Figures 2D–2F), suggesting that APPL1 potentiates the hepatic actions of insulin on inhibiting glucose production via Akt activation.

Hepatic Silencing of APPL1 Decreases Insulin Sensitivity and Glucose Tolerance in Mice

To investigate the effects of APPL1 on hepatic insulin sensitivity in vivo, we injected C57BL/6J mice with adenovirus encoding APPL1-specific siRNA to reduce its expression in the liver. Western blot analysis showed a time-dependent decrease in APPL1 expression in the liver after injection with adenoviruses (Figure 3A). On days 5 and 8 after adenoviral infection, the protein abundance of APPL1 was decreased by approximately 79% and 65%, respectively, compared to the scrambled control group. Afterward, the knockdown efficiency was gradually diminished.

Knockdown of APPL1 in the liver did not affect food intake and body weight gains (data not shown), but significantly increased

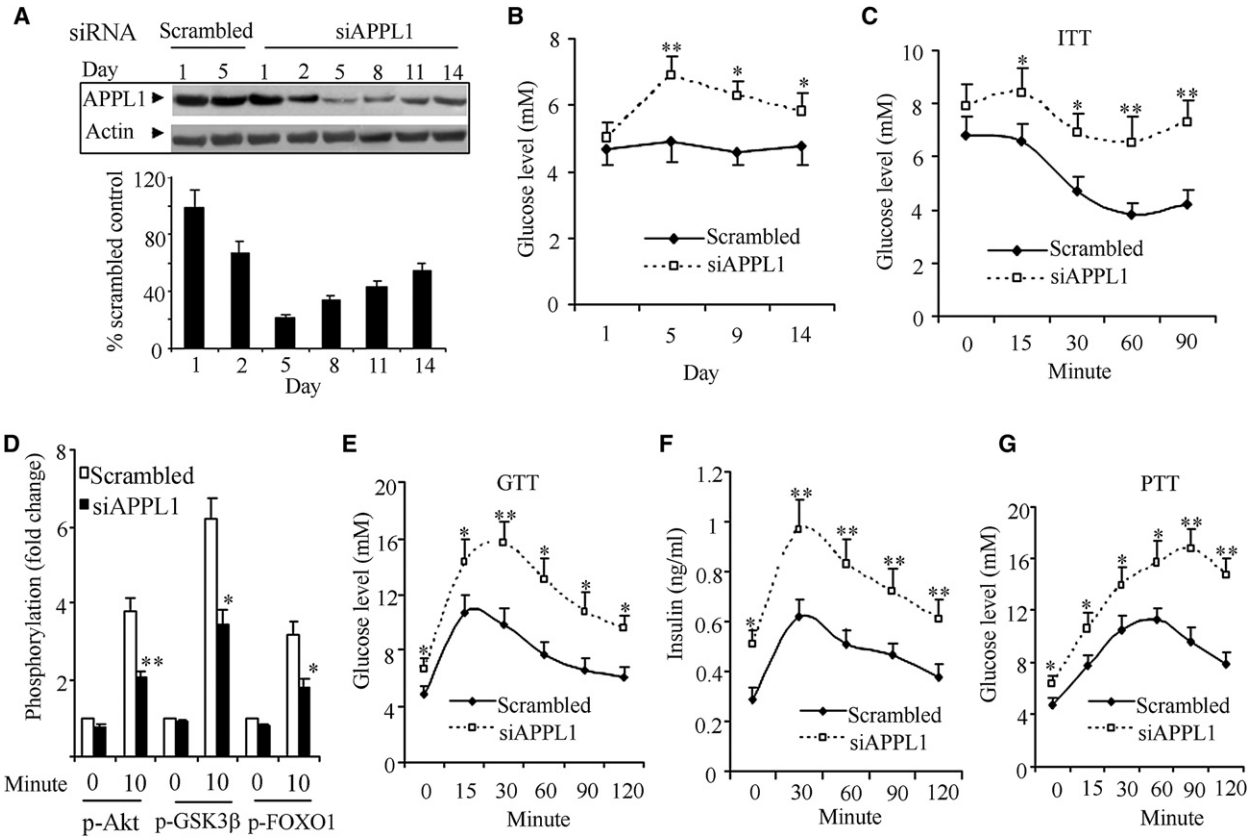

Figure 3. Knockdown of APPL1 Expression by siRNA Impairs the Hepatic Actions of Insulin and Induces Hyperglycemia in C57 Mice

Ten-week-old C57 male mice were treated with adenovirus encoding APPL1 siRNA (siAPPL1) or scrambled control by tail vein injection (2×10^9 p.f.u./mouse).

(A) Western blot analysis to detect protein levels of APPL1 in the liver tissue of mice at various days after adenoviral infection. The bar chart below the blot is the quantitative analysis of APPL1 protein abundance.

(B) Fasting glucose levels at various days after adenoviral infection.

(C) Insulin tolerance test (ITT) on day 9.

(D) Phosphorylation of Akt and its two targets in response to acute insulin injection (0.5 IU insulin/kg body weight) on day 10. Data are expressed as fold changes relative to the baseline control (time = 0 min).

(E) Glucose tolerance test (GTT) on day 6.

(F) Circulating levels of insulin at various time points during the glucose tolerance test on day 6.

(G) Pyruvate tolerance test (PTT) on day 7.

Error bars are ±SEM. *$p < 0.05$; **$p < 0.01$ (n = 5–7).

plasma levels of fasting glucose (Figure 3B). The most profound elevation of fasting glucose was detected on day 5, which was in parallel with the greatest reduction in APPL1 expression. Insulin tolerance test, conducted at day 9 after adenoviral injection, showed significantly decreased insulin sensitivity in mice with reduced APPL1 expression, as evidenced by a much greater area under the glucose curve compared to scrambled control (Figure 3C). These changes during APPL1 knockdown was accompanied at a molecular level by decreased phosphorylation of Akt and its two downstream targets GSK3β and FOXO1 in response to acute intraperitoneal insulin injection (Figure 3D), a finding consistent with the observation in isolated hepatocytes (Figure 1).

Glucose tolerance test, conducted at day 6 after infusion with recombinant adenoviruses, showed that knockdown of APPL1 expression in the liver caused a significant impairment in glucose excursion after glucose challenge (Figure 3E). Noticeably, insulin levels at both baseline and during glucose tolerance test were elevated in mice with reduced APPL1 expression in the liver (Figure 4F). The effect of APPL1 knockdown on inducing glucose intolerance was insignificant at day 13 (data not shown), perhaps due to the decreased knockdown efficiency and/or the compensatory increase of circulating insulin, thus leading to an increased glucose disposal in other insulin targets such as skeletal muscle and adipocytes.

To determine the role of APPL1 in modulating gluconeogenesis in vivo, we also examined blood glucose levels in mice following intraperitoneal injection of pyruvate in a separate set of experiments (Figure 3G). In control mice, blood glucose increased to a peak level at 60 min after pyruvate administration, and decreased afterward. However, in mice with reduced APPL1 expression, blood glucose continued to rise at 90 min, and did not significantly decrease until 120 min. Compared to the mice infected with scrambled control, the glucose area after pyruvate challenge was much greater in mice infected with adenovirus encoding APPL1-specific siRNA.

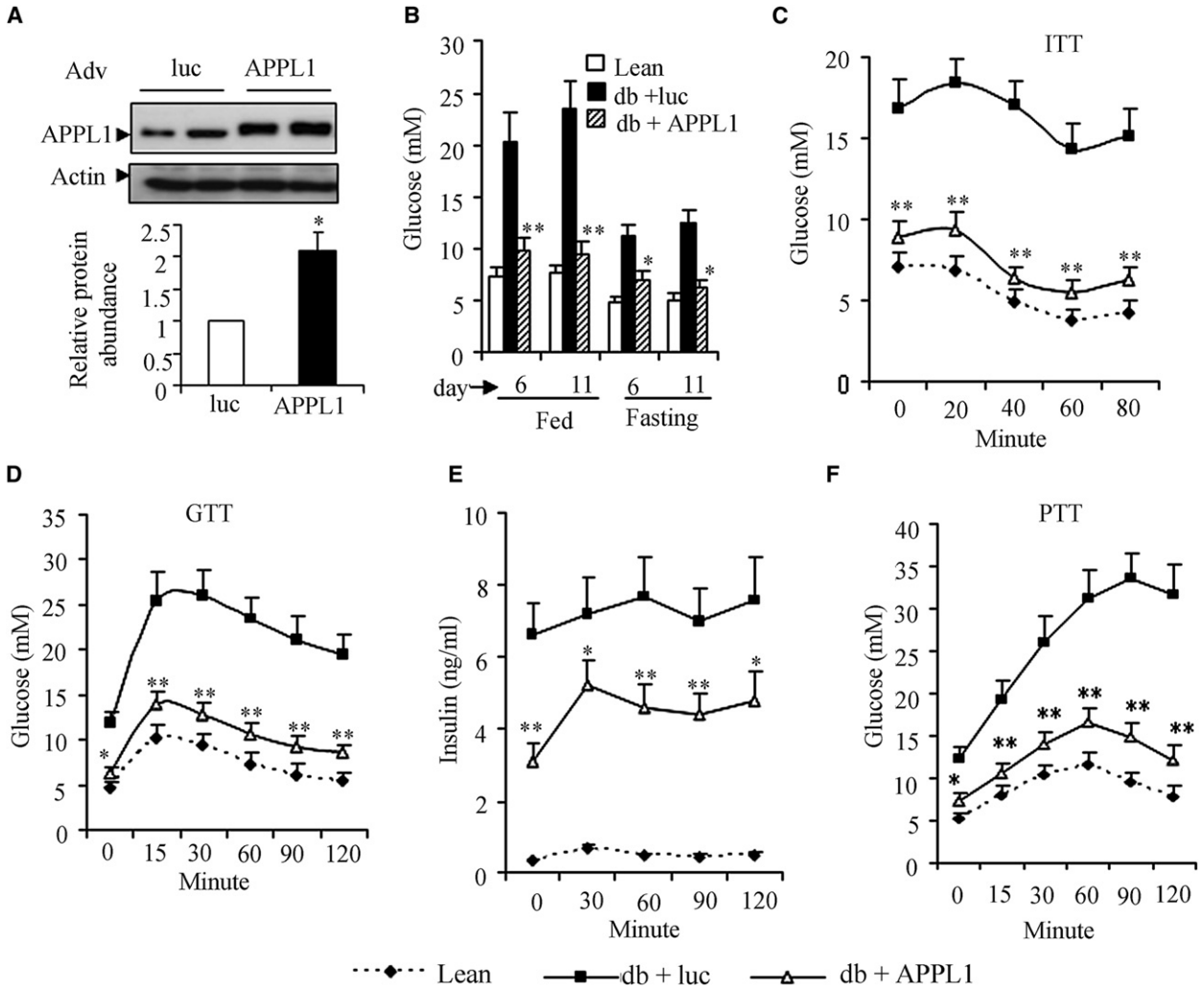

Figure 4. Adenovirus-Mediated Expression of APPL1 Alleviates Diabetic Phenotype in *db/db* Obese Mice

(A) Immunoblot analysis to detect the protein levels of APPL1 in the liver tissue of *db/db* mice at day 16 after infection with adenovirus (Adv) encoding APPL1 or luciferase (luc) control (2×10^9 p.f.u./mouse).

(B) Fed and fasting blood glucose levels on day 6 and day 11 after adenoviral injection.

(C) Insulin tolerance test on day 11.

(D) Glucose tolerance test on day 8.

(E) Serum levels of insulin at various time points after glucose challenge on day 8.

(F) Pyruvate tolerance test on day 6 after adenoviral treatment. Note that the data from age-matched db/+ lean littermates are also presented in (B)–(F) for the purpose of comparison.

Error bars are ±SEM. *$p < 0.05$; **$p < 0.01$ versus *db/db* +luc group (n = 5–6).

Hepatic Overexpression of APPL1 Alleviates Hyperglycemia and Insulin Resistance in Obese Mice

To further confirm the insulin-sensitizing effects of APPL1 in an in vivo setting, we evaluated the metabolic changes in *db/db* obese mice with frank diabetes following adenovirus-mediated APPL1 overexpression. The ectopic expression of APPL1 in the liver tissue of these mice was detectable at day 3, and was still present at day 16 after initial injection (Figure 4A). As expected, infusion of adenovirus via tail vein injection did not affect APPL1 expression in any other tissues examined, including muscle and adipose tissue (data not shown).

Overexpression of APPL1 in the liver caused a significant amelioration of both fasting and fed hyperglycemia in *db/db* diabetic mice, restoring them to nearly normal values observed in lean littermates (Figure 4B). Insulin tolerance and glucose tolerance tests showed that adenovirus-mediated APPL1 overexpression led to obvious alleviations in both insulin resistance and glucose intolerance in *db/db* mice, as evidenced by much smaller areas under the glucose curves compared to those infused with adenovirus encoding luciferase control (Figures 4C and 4D). In *db/db* mice with APPL1 overexpression, circulating insulin levels at both baseline (16 hr after starvation) and various time points during glucose challenge were much lower than those in the luciferase control group (Figure 4E). Pyruvate tolerance test showed that APPL1 overexpression decreased pyruvate-induced gluconeogenesis to a level close to that observed in lean littermates (Figure 4F).

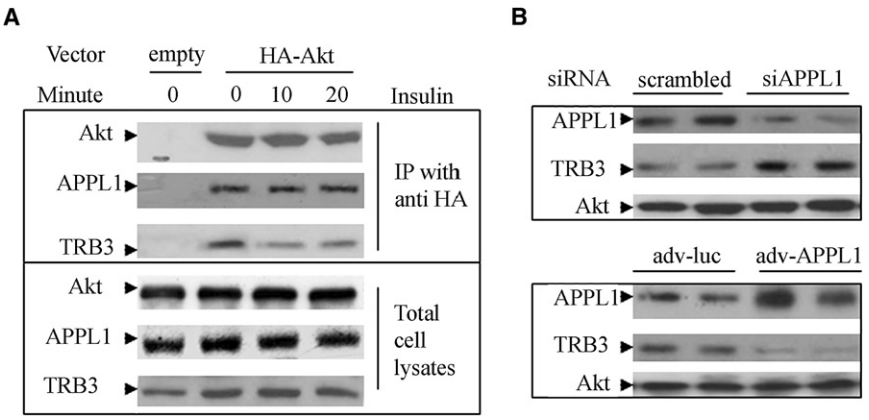

Figure 5. APPL1 Modulates the Interaction between Akt and TRB3 in Hepatocytes

(A) Rat hepatocytes were transfected with a plasmid encoding HA-tagged Akt or an empty vector for 48 hr, and then treated with 10 nM insulin for various periods. Cell lysates were subjected to immunoprecipitation with anti-HA antibody, and then probed with anti-TRB3, anti-APPL1, or anti-Akt, as indicated.

(B) Cells were infected with adenovirus encoding APPL1 or luciferase, or APPL1-specific siRNA (siAPPL1) or scrambled control as indicated for 6 hr, and subsequently transfected with a plasmid encoding HA-tagged Akt. Cell lysates harvested at 48 hr after transfection were subjected to immunoprecipitation and immunoblot analysis as in (A).

Consistent with our finding in primary rat hepatocytes, adenovirus-mediated APPL1 overexpression significantly increased Akt phosphorylation at Ser-473 after either insulin or glucose administration in *db/db* mice (Figure S2). Glycogen content in the liver tissue, as determined by both histological and enzymatic methods, was significantly elevated by APPL1 overexpression (Figures S3A and S3B). By contrast, APPL1 had no obvious effect on hepatic lipid content, as evaluated by oil red O staining and biochemical analysis (Figures S3C and S3D).

Adenovirus-mediated overexpression of APPL1 also led to significant alleviations in insulin resistance and glucose intolerance in high-fat diet-induced obese mice (data not shown).

APPL1 Does Not Affect Insulin-Evoked Signaling Events Upstream of Akt

Insulin induces Akt activation by stimulating tyrosine phosphorylation of IRS1 and IRS2, which in turn triggers activation of phosphoinositide-3-kinase (PI3K) and phosphoinositide-dependent kinase 1 (PDK1). We next investigated whether APPL1 regulates these upstream signaling events in the liver tissue of C57 mice (Figure S4). Although adenovirus-mediated knockdown of APPL1 impaired insulin-evoked Akt activation in the liver (Figure 3), it had no obvious effect on either the protein levels or insulin-elicited tyrosine phosphorylation of IRS1 and IRS2, or on insulin-induced elevation of PI3K activity (Figures S4A and S4B). Suppression of APPL1 expression by siRNA did not alter either the protein abundance or the activity of PDK1 under either basal condition or 10 min after insulin administration (Figure S4C), or on its subcellular localization (data not shown). In addition, knockdown of APPL1 expression did not alter the protein abundance of protein phosphatase 2A (PP2A) or its enzyme activity at either baseline or 10 min after insulin administration (Figure S4D). Adenovirus-mediated overexpression of APPL1 in the liver of *db/db* mice also had no obvious impact on insulin-induced phosphorylation of IRS1 and IRS2, or on the activity of PI3K, PDK1, or PP2A (data not shown).

APPL1 Blocks the Interaction between Akt and TBR3

Several previous studies have shown a direct interaction of APPL1 with Akt (Mitsuuchi et al., 1999; Saito et al., 2007; Yang et al., 2003). It is well established that the activity of Akt can be modulated via its interaction with various binding partners. In particular, the pseudokinase tribble 3 (TRB3) binds to Akt and prevents insulin-mediated Akt phosphorylation by its upstream kinases (Du et al., 2003; Koo et al., 2004). Interestingly, although both APPL1 and TRB3 interact with Akt, the two proteins exert opposite effects on phosphorylation of Akt. We therefore investigated the effect of APPL1 on the interactions between TRB3 and Akt2, a major isoform responsible for the metabolic actions of insulin (Cho et al., 2001). Immunoprecipitation analysis detected the association of Akt with both APPL1 and TRB3 under the basal condition (Figure 5A). Insulin stimulation did not have obvious effects on the interaction between APPL1 and Akt, but attenuated the association between Akt and TRB3. Notably, the association of Akt with TRB3 was markedly enhanced by knockdown of APPL1 expression, but was suppressed by APPL1 overexpression (Figure 5B). These findings raise the possibility that APPL1 potentiates insulin-induced Akt activation by blocking its association with TRB3.

To address the physiological relevance of the above findings, we further investigated the interplay between Akt, APPL1, and TRB3 in mouse livers. Consistent with a previous report (Du et al., 2003), our western blot analysis showed a much higher protein level of TRB3 in the liver tissue of *db/db* mice compared to that in wild-type littermates, whereas the expression levels of Akt and APPL1 were comparable between the two groups (Figure S5A). Interestingly, coimmunoprecipitation analysis detected a significantly elevated association between Akt and TRB3, and a decreased association between Akt and APPL1 in the liver tissue of *db/db* obese mice (Figure S5B). In high-fat diet-induced obese mice and KK-Ay obese mice, we also observed an increased association of Akt with TRB3 and a decreased association of Akt with APPL1 compared to lean littermates (data not shown). Importantly, overexpression of APPL1 in the liver of *db/db* obese mice suppressed the interaction between Akt and TRB3 (Figure S5C).

APPL1 Counteracts the Inhibitory Effects of TRB3 on Insulin-Induced Akt Signaling

To further elucidate the molecular basis whereby APPL1 inhibits the interaction between TRB3 and Akt, we established in vitro pull-down assays using recombinant TRB3 tagged with glutathione S-transferase (GST-TRB3) and APPL1 tagged with six histidines (His-APPL1) at their NH_2 termini. This analysis showed that endogenous Akt from primary rat hepatocytes bound robustly to recombinant GST-TRB3 (Figure S6A), but not GST

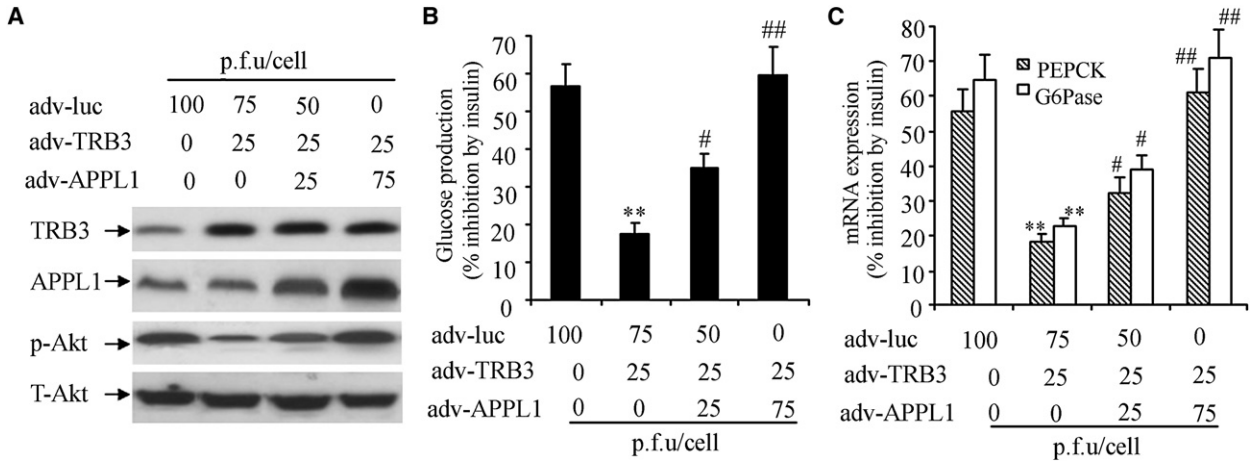

Figure 6. APPL1 Antagonizes the Inhibitory Effect of TRB3 on Insulin-Induced Akt Phosphorylation and Suppression of the Gluconeogenic Program in Primary Rat Hepatocytes

(A) Cells were infected with adenovirus encoding luciferase (adv-luc), TRB3 (adv-TRB3), and/or APPL1 (adv-APPL1) at the concentrations (p.f.u./cell) indicated. At 36 hr after adenoviral infection, cells were starved for another 12 hr, and stimulated with 10 nM insulin for various periods, as indicated. Cell lysates were subjected to western blot analysis using anti-TRB3, -APPL1, -phospho-, and -total Akt, as specified.

(B and C) The effects of insulin on cAMP/Dex-induced glucose production and expression of the two gluconeogenic genes were analyzed as in Figure 2. The data are presented as percentage of inhibition by insulin relative to cells treated with cAMP/Dex alone. Error bars are ±SEM. **$p < 0.01$ versus the group infected with adv-luc only; #, $p < 0.05$; ##, $p < 0.01$ versus the group infected with adv-TRB3 (25 p.f.u./cell) plus adv-luc (75 p.f.u./cell). n = 5–6 in each group.

alone. The binding of Akt to GST-TRB3 was abolished by adenovirus-mediated overexpression of APPL1, or by direct addition of purified recombinant APPL1 into the in vitro reaction mixture. Conversely, the interaction between Akt and purified His-APPL1 was largely attenuated by either adenovirus-mediated overexpression of TRB3 or by incubation with an excessive amount of recombinant GST-TRB3 (Figure S6B). Consistent with the results from the pull-down analysis, our gel overlay assay (far western) further confirmed that TRB3 interacted directly with Akt preimmobilized on the nitrocellulose membranes, and this interaction was blocked by coincubation with an excessive amount of recombinant His-APPL1 (Figure S6C). By contrast, recombinant APPL1 bound to the immobilized Akt under both basal and insulin-stimulated conditions, and this interaction was attenuated by adding an excessive amount of recombinant GST-TRB3 to the incubation buffer (Figure S6D). These results suggest that APPL1 and TRB3 bind to Akt in a competitive manner.

We next investigated the interplay between APPL1 and TRB3 on insulin-evoked Akt signaling in primary rat hepatocytes. Consistent with the previous finding (Du et al., 2003), adenovirus-mediated overexpression of TRB3 led to a significant reduction in insulin-evoked phosphorylation of Akt, and attenuated the ability of insulin to suppress the expression of gluconeogenic genes and glucose production induced by cAMP/Dex (Figure 6). This inhibitory effect of TRB3 on insulin-induced Akt phosphorylation and suppression of the gluconeogenic program was abolished by adenovirus-mediated elevation of APPL1 expression in a dose-dependent manner, suggesting that APPL1 can directly antagonize the insulin-desensitizing effects of TRB3 on Akt signaling.

APPL1 and TRB3 Exert Opposite Effects on the Subcellular Distribution of Akt

The diversity and specificity of insulin signal transduction are accomplished in part by spatial compartmentalization of key signaling components. Although the plasma membrane is traditionally thought to be a major site for Akt activation, a growing body of evidence suggests that trafficking through the endosomal apparatus is also important for achieving full activation of insulin-evoked Akt signaling (Su et al., 2006). Insulin has been reported to induce the endosomal localization of Akt as well as its upstream components such as PI3K (Balbis et al., 2000). A recent study on zebrafish demonstrates that the potentiating effect of APPL1 on Akt activation occurs within the endosomes (Schenck et al., 2008). We therefore investigated the effects of APPL1 on subcellular distribution of Akt in well-defined subcellular fractions (cytosol, plasma membrane, and endosomes) from the liver of C57 mice. Under the fasting condition, Akt was present predominantly in the cytosol in an inactive form (Figure 7A). A small portion of Akt was also detectable in the endosomes, but not in the plasma membrane. APPL1 was evenly distributed in the cytosol and in the endosomes. Insulin stimulation induced the translocation of Akt to the plasma membrane as well as the endosomes. Interestingly, insulin-induced Akt translocation to the endosomes was accompanied by increased accumulation of APPL1 in this compartment. Furthermore, insulin-stimulated Akt translocation to the endosomes in mouse livers was markedly elevated by APPL1 overexpression (Figure 7B), but decreased by knockdown of APPL1 expression (Figure 7C). Insulin-induced Akt translocation to the plasma membrane was also reduced by APPL1 knockdown and was elevated by APPL1 overexpression, whereas the magnitude of these changes was much smaller than that in the endosomes.

TRB3 was found exclusively in the cytosolic fraction under both basal and insulin-stimulated conditions (Figure 7A). Knockdown or overexpression of APPL1 had no effect on intracellular localization of TRB3 (data not shown). Noticeably, overexpression of TRB3 in the liver tissue of C57 mice blocked insulin-evoked

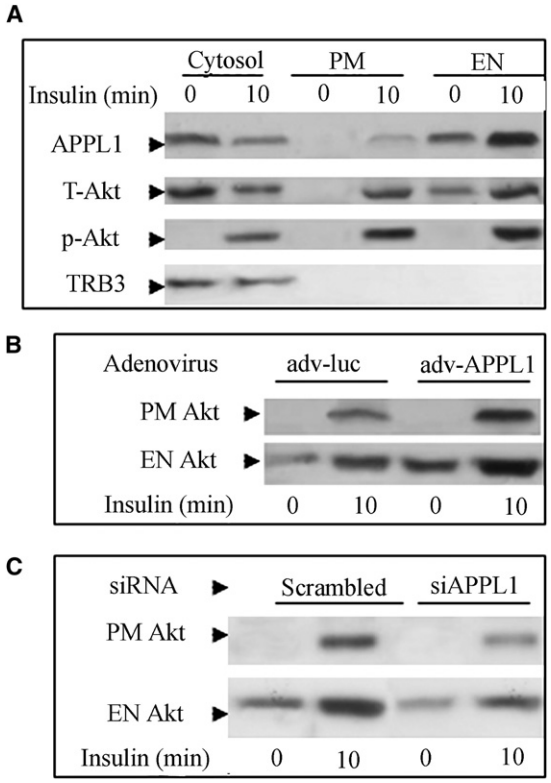

Figure 7. APPL1 Promotes Insulin-Evoked Akt Recruitment to the Endosomes and the Plasma Membrane

(A) Subcellular distribution of Akt, APPL1, and TRB3 in mouse liver under basal and insulin-stimulated conditions. Mice were fasted overnight, and sacrificed after receiving a single injection of insulin for 0 or 10 min. Aliquots (40 μg protein) of the plasma membrane (PM), endosomes (EN), and cytosol purified from the liver of these mice were subjected to immunoblotting analysis using various antibodies, as indicated.

(B and C) C57 male mice were injected with adenovirus encoding APPL1 (adv-APPL1) or luciferase (adv-luc), or adenovirus encoding APPL1 siRNA (siAPPL1) or scrambled control, as indicated. On day 10 after injection, mice were fasted overnight, received a single injection of insulin, and then sacrificed to obtain liver tissue for subcellular fractionation as in (A). Aliquots (40 μg protein) of EN and PM fractions were subjected to western blot analysis using anti-total Akt.

translocation of Akt to the endosomes as well as the plasma membrane (Figure S7).

DISCUSSION

This study provides both ex vivo and in vivo evidence showing that APPL1 can potentiate the hepatic actions of insulin on suppressing glucose production through Akt activation. In primary hepatocytes, insulin-evoked phosphorylation of Akt and its downstream targets and inhibition of the gluconeogenic program are markedly attenuated by knockdown of APPL1 expression, but enhanced by its overexpression. The physiological relevance of APPL1 as a key regulator of insulin signaling is also supported by both loss-of-function and gain-of-function studies in animal models. Most strikingly, selective overexpression of APPL1 in the liver causes an almost complete reversal of hyperglycemia, insulin resistance, and glucose intolerance in *db/db* obese mice, suggesting that APPL1 might represent a potential therapeutic target for the treatment and/or prevention of hepatic insulin resistance and T2DM.

Several recent reports have shown that APPL1 interacts with and activates Akt (Liu et al., 2002; Saito et al., 2007; Yang et al., 2003). However, the underlying mechanisms have yet to be explored. In this study, we demonstrate that APPL1 does not play a role in modulating insulin-induced signaling events upstream of Akt. Instead, the potentiating effect of APPL1 on insulin-induced Akt activation is attributed in part to its ability in blocking the association of Akt with its endogenous inhibitor TRB3. In several insulin target tissues including hepatocytes, myotubes, and endothelium, TRB3 interacts with Akt and prevents Akt phosphorylation by its upstream kinases (Andreozzi et al., 2008; Du et al., 2003; Kato and Du, 2007). In addition, TRB3 blocks insulin-stimulated Akt translocation to the plasma membrane by its direct interaction with Akt (He et al., 2006). Elevated TRB3 expression has previously been implicated as a mediator of insulin desensitization in the liver tissue of *db/db* obese mice (Du et al., 2003) as well as in several other insulin-resistant conditions (He et al., 2006; Koo et al., 2004). Noticeably, hepatic overexpression of TRB3 in amounts comparable to those in *db/db* mice promotes hyperglycemia and insulin resistance, whereas knocking down its expression improves insulin sensitivity in *db/db* mice (Du et al., 2003). Our present study shows that APPL1 inhibits the interaction between Akt and TRB3 in primary hepatocytes as well as in mouse liver tissue, which is accompanied by increased membrane translocation and enhanced activation of Akt in response to insulin stimulation. Both our in vitro pull-down assay and far western analysis demonstrate that APPL1 directly competes with TRB3 for binding to Akt. Furthermore, overexpression of APPL1 can counteract the inhibitory effect of TRB3 on insulin-evoked Akt activation and suppression of the gluconeogenic program in rat hepatocytes. These findings suggest that insulin-mediated Akt activation is finely tuned by the relative expression level of TRB3 and APPL1, and their binding to this kinase.

Although the protein level of APPL1 remains unchanged in obese mice with insulin resistance, we observed a significantly decreased Akt association with APPL1 and an increased Akt association with TRB3 compared to the lean control mice, perhaps due to the elevated expression of TRB3. Noticeably, blockage of the augmented interaction between Akt and TRB3 in the liver of *db/db* obese mice by hepatic overexpression of APPL1 is paralleled by a marked alleviation of hyperglycemia and insulin resistance. These findings raise the possibility that the imbalance in Akt association with APPL1 and TRB3 may contribute to hepatic insulin resistance in *db/db* obese mice. The antidiabetic actions of APPL1 observed in *db/db* mice can be explained in part by its counteracting effect against elevated inhibition of TRB3 on Akt activation.

Another notable observation of the present study is the ability of APPL1 to promote insulin-evoked translocation of Akt to the endosomal compartment. In line with a previous report (Balbis et al., 2000), our subcellular fraction analysis shows that insulin stimulates Akt translocation to the plasma membrane as well as to the endosomes in mouse liver. Furthermore, insulin-evoked endosomal recruitment of Akt is associated with increased APPL1 translocation to this compartment. In addition to the

plasma membrane, the endosomal compartment has recently been implicated as an important site for achieving full Akt activation by insulin as well as for determining the substrate specificity of this insulin signaling pathway. The activated insulin receptor kinase complexes are rapidly internalized into the endosomes upon insulin stimulation (Fiory et al., 2004). The endosomal compartment is the important site for IRS1 phosphorylation, recruitment, and activation of PI3K subunits in adipocytes (Inoue et al., 1996; Nave et al., 1996). Subcellular fractionation analysis has demonstrated that insulin-stimulated membrane recruitment of p85 (the regulatory subunit of PI3K) occurs predominantly in the microsomal fraction enriched with the endosomes, but not in the plasma membrane fraction (Nave et al., 1996). Noticeably, a key role of the endosomal compartment in the insulin-evoked Akt signaling cascade is highlighted by several recent reports showing that knockdown of the small GTPase Rab5, a major regulator of endocytosis, blocks insulin-stimulated activation of Akt as well as glucose uptake in adipocytes (Su et al., 2006; Huang et al., 2001). APPL1 is a downstream effector protein of Rab5 (Miaczynska et al., 2004). A large portion of APPL1 is colocalized with Rab5 in the endosomal compartment (Miaczynska et al., 2004). In zebrafish, APPL1-mediated Akt activation occurs predominantly within the endosomes where some Akt substrates (such as GSK3) are also available (Schenck et al., 2008). Consistent with these zebrafish-based observations, the present study also shows that APPL1-mediated potentiation of Akt activation by insulin results in a markedly enhanced GSK3β phosphorylation and increased glycogen accumulation in mouse liver.

The detailed molecular mechanism by which the interplay between APPL1 and TRB3 modulates insulin-mediated Akt activation remains to be determined. Importantly, our results demonstrate that APPL1 and TRB3 exhibit a distinct pattern of subcellular distribution and possess opposite effects on the membrane translocation of Akt. TRB3 is predominantly at the cytosolic fraction of liver tissue and is virtually undetectable in the endosome and plasma membrane even after insulin stimulation. Overexpression of TRB3 arrests Akt in the cytosol and prevents insulin-induced Akt translocation to the endosomes and the plasma membrane. In contrast to TRB3, insulin stimulation causes the redistribution of APPL1 from the cytosol to the endosomes as well as the plasma membrane. Furthermore, APPL1 also promotes insulin-induced Akt translocation from the cytosol to the endosomes and plasma membrane. Taken in conjunction, these data suggest that insulin-mediated Akt activation is finely tuned by APPL1 and TRB3 through spatial regulation. TRB3 inhibits Akt activation by arresting it at the cytosol and blocking its membrane translocation. By contrast, APPL1 competes with TRB3 for binding to Akt, subsequently promoting Akt translocation to the cell membrane for further activation.

Besides binding to Akt, APPL1 also interacts with several other molecules involved in signaling transduction, including both regulatory (p85) and catalytic (p110) subunits of PI3K (Mitsuuchi et al., 1999), Rab5, GIPC (Varsano et al., 2006), and inositol 5-phosphatase (Erdmann et al., 2007). In addition, APPL1 possesses phosphoinositide-binding properties (Chial et al., 2008; Li et al., 2007a). Our present study does not exclude the possibility that the interactions between APPL1 with these signaling components also contribute to the potentiating effects of APPL1 on Akt activation. Further detailed analysis of the molecular basis underlying the potentiating effects of APPL1 on insulin-evoked activation of the Akt signaling cascade might shed new light on the fundamental mechanism whereby insulin controls glucose homeostasis.

EXPERIMENTAL PROCEDURES

Antibodies and Chemicals

Rabbit polyclonal antibodies against total Akt, phospho-Akt (Ser-473), total GSK3β, phospho-GSK3β (Ser-9), total FOXO1, and phospho-FOXO1 (Ser-256) were from Cell Signaling Technology, and antibodies against IRS1 and IRS2, and anti-phosphotyrosine (Tyr[P]) were purchased from Upstate Biotechnology. Goat anti-Akt2 IgG was from Symansis. Rabbit anti-TRB3 and anti-HA antibodies were from Calbiochem. Insulin, dexamethasone, cAMP, PP2 (4-amino-5-[4-chlorophenyl]-7-[*t*-butyl]pyrazolo[3,4-d]pyrimidine) and PP3 (4-amino-7-phenylpyrazolo[3,4-d]pyrimidine] were from Sigma. [γ-^{32}P]ATP was from Amersham.

Animal Experiments

C57BL/6J male mice and Wistar male rats were purchased from the animal unit of The University of Hong Kong. Twelve-week-old male C57BL/KsJ-lepr(db)/lepr(db) obese/diabetic mice and age-matched lean littermate db/+ mice were originally obtained from Jackson Laboratories. The mice were housed in a room under controlled temperature (23°C ± 1°C) with free access to water and standard chow. Glucose tolerance and insulin tolerance tests were conducted as we previously described (Xu et al., 2005). Serum levels of insulin were quantified using an ELISA kit from Mercodia AB (Uppsala, Sweden). Pyruvate tolerance test was performed to estimate gluconeogenesis as follows. Mice were starved for 16 hr, and then injected intraperitoneally with pyruvate (2 g/kg) dissolved in saline. Blood glucose levels were determined in tail blood every 30 min for 2 hr using the Ascensia Elite XL blood glucose meter (Bayer Health Care). All of the experiments were conducted under our institutional guidelines for the humane treatment of laboratory animals.

Construction of Adenoviral Vectors for Knockdown or Overexpression of APPL1

An adenovirus-mediated small hairpin RNAi delivery system was used to knock down APPL1 expression. The oligonucleotides against APPL1 and scrambled control are listed in Table S1. The forward and reverse oligonucleotides were annealed, ligated into pENTR/U6 entry vector, and then subcloned into pAd/BLOCK-iT DEST vector through recombination. To construct adenoviral vectors for overexpression of APPL1 or TRB3, cDNA encoding full-length human APPL1 or TRB3 was inserted into pshuttle-CMV vector, and then subcloned into pAdeasy-1 adenoviral backbone vector (Stratagene) through recombination in *Escherichia coli*.

To package adenovirus, the adenoviral vectors were linearized with the restriction enzyme PacI and transfected into HEK293 cells using Lipofectamine 2000. After several rounds of propagation, recombinant adenovirus was purified by an AdEasy virus purification kit (Stratagene), and the titer was determined with an endpoint assay as described (Xu et al., 2005).

Isolation of Primary Rat Hepatocytes, Cell Culture, and Measurement of Glucose Production

Primary hepatocytes were prepared from male Wistar rats (~200 g) which have been fasted for 16 hr as described (Wang et al., 2002). Cells were plated on collagen type I-coated 12-well plates in Dulbecco's modified Eagle's medium (DMEM) with 10% fetal bovine serum at a density of 5×10^5 cells per well, and then transduced with various adenoviruses for 48 hr. Thereafter, cells were washed three times with warm PBS to remove glucose, pretreated with insulin, followed by stimulation with cAMP/dexamethasone in glucose-free DMEM containing gluconeogenic substrates (2 mM sodium pyruvate). Glucose concentrations were determined with a glucose assay kit from Sigma.

Subcellular Fractionation

Rat primary hepatocytes grown in 35 mm culture dishes (1.5×10^6) were rinsed with ice-cold PBS, and dissolved with a lysis buffer containing 20 mM

Tris-Cl (pH 7.5), 150 mM NaCl, 1 mM Na_2EDTA, 1 mM EGTA, 1% Triton X-100, 2.5 mM sodium pyrophosphate, 1 mM β-glycerophosphate, 1 mM Na_3VO_4, and protease inhibitor cocktails (Roche, Mannheim, Germany). Cytoplasmic and nuclear fractions were prepared using NE-PER nuclear and cytoplasmic extraction reagents according to the manufacturer's instruction (Pierce).

C57 mice fasted overnight were anesthetized and killed at various times after insulin injection. Livers were rapidly excised, minced in an ice-cold buffer consisting of 250 mM sucrose, 4 mM imidazole (pH 7.4) plus protease inhibitor cocktails and phosphatase inhibitors (2 mM sodium fluoride and 1 mM sodium orthovanadate), and homogenized using a teflon pestle. The cytosol, plasma membrane, and endosomal fractions were isolated from the liver homogenates using discontinuous sucrose-gradient ultracentrifugation as described previously (Balbis et al., 2000; Khan et al., 1989).

Immunoprecipitation and Immunoblotting

Immunoprecipitation was conducted as described previously (Cheng et al., 2007). Proteins from total cell lysates, various subcellular fractions, or immunoprecipitated complexes were separated by SDS-PAGE, and probed with different primary antibodies as specified in each figure legend. The specific signals were amplified by addition of horseradish peroxidase-conjugated secondary antibodies and visualized using an enhanced chemiluminescence system (Amersham). The intensity of the protein bands was quantified using an image processor program (ImageJ).

Hepatic Glycogen and Triglyceride Contents

The cryostat sections of mouse livers obtained after 6 hr of fasting were deparaffinized by incubating with xylene for 5 min, hydrated, and then oxidized in 0.5% periodic acid solution for 5 min. After washing with distilled water, the sections were incubated with periodic acid Schiff (Sigma) prior to imaging. The glycogen concentrations in liver were also quantified using an enzymatic method as follows. Frozen liver tissue (20–30 mg) was dissolved in 1 M NaOH at 65°C for 1 hr, spotted onto Whatman 3M paper, dried, and washed three times with 65% ethanol. The samples were then digested with amyloglucosidase at 45°C for 4 hr and glucose content was measured with a glucose oxidase assay. Oil red O staining of lipid droplets in liver sections and enzymatic quantification of hepatic triglyceride contents in the liver tissue were performed as described (Xu et al., 2005).

RNA Extraction and Real-Time PCR

Total RNA from rat hepatocytes or mouse liver tissue was purified with a Trizol reagent (Invitrogen), and treated with RNase-free DNase (Promega) at 37°C for 30 min to remove genomic DNA. For reverse transcription, 1 μg of the total RNA was converted to first-strand complementary DNA in 20 μl reactions using a cDNA synthesis kit (Promega). Quantitative real-time PCR for mRNA expression of the two gluconeogenic genes was performed in duplicate in a total reaction volume of 20 μl with a fluorescent TaqMan 5′-nuclease assay on an Applied Biosystems Prism 7000 sequence detection system (assay ID: Mm00440636_m1 for *PEPCK* and Mm00839363_m1 for *G6Pase*). Analysis was performed with ABI Prism 7000 SDS software and normalized against 18S RNA.

Statistical Analysis

Experiments were performed routinely with four to six mice per group with values presented as means ± standard error. Statistical significance was determined by one-way ANOVA or Student's t test. In all statistical comparisons, p value < 0.05 was used to indicate a significant difference.

SUPPLEMENTAL DATA

Supplemental data include Supplemental Experimental Procedures, one table, and seven figures and can be found with this article online at http://www.cell.com/cell-metabolism/supplemental/S1550-4131(09)00091-6.

ACKNOWLEDGMENTS

This work was supported by the general research fund (HKU 779707M to A.X.) and collaborative research fund (HKU 2/07C) from the Research Grants Council of Hong Kong, the National 973 Program of China (2006CB503908), and the National Health and Medical Research Council of Australia (to E.W.K.).

Received: October 22, 2008
Revised: February 6, 2009
Accepted: March 31, 2009
Published: May 5, 2009

REFERENCES

Accili, D. (2004). Lilly lecture 2003: the struggle for mastery in insulin action: from triumvirate to republic. Diabetes *53*, 1633–1642.

Andreozzi, F., Formoso, G., Prudente, S., Hribal, M.L., Pandolfi, A., Bellacchio, E., Di Silvestre, S., Trischitta, V., Consoli, A., and Sesti, G. (2008). TRIB3 R84 variant is associated with impaired insulin-mediated nitric oxide production in human endothelial cells. Arterioscler. Thromb. Vasc. Biol. *28*, 1355–1360.

Balbis, A., Baquiran, G., Bergeron, J.J., and Posner, B.I. (2000). Compartmentalization and insulin-induced translocations of insulin receptor substrates, phosphatidylinositol 3-kinase, and protein kinase B in rat liver. Endocrinology *141*, 4041–4049.

Barthel, A., and Schmoll, D. (2003). Novel concepts in insulin regulation of hepatic gluconeogenesis. Am. J. Physiol. Endocrinol. Metab. *285*, E685–E692.

Biddinger, S.B., and Kahn, C.R. (2006). From mice to men: insights into the insulin resistance syndromes. Annu. Rev. Physiol. *68*, 123–158.

Cheng, K.K., Lam, K.S., Wang, Y., Huang, Y., Carling, D., Wu, D., Wong, C., and Xu, A. (2007). Adiponectin-induced endothelial nitric oxide synthase activation and nitric oxide production are mediated by APPL1 in endothelial cells. Diabetes *56*, 1387–1394.

Chial, H.J., Wu, R., Ustach, C.V., McPhail, L.C., Mobley, W.C., and Chen, Y.Q. (2008). Membrane targeting by APPL1 and APPL2: dynamic scaffolds that oligomerize and bind phosphoinositides. Traffic *9*, 215–229.

Cho, H., Mu, J., Kim, J.K., Thorvaldsen, J.L., Chu, Q., Crenshaw, E.B., III, Kaestner, K.H., Bartolomei, M.S., Shulman, G.I., and Birnbaum, M.J. (2001). Insulin resistance and a diabetes mellitus-like syndrome in mice lacking the protein kinase Akt2 (PKB β). Science *292*, 1728–1731.

Dentin, R., Liu, Y., Koo, S.H., Hedrick, S., Vargas, T., Heredia, J., Yates, J., III, and Montminy, M. (2007). Insulin modulates gluconeogenesis by inhibition of the coactivator TORC2. Nature *449*, 366–369.

Dong, X.C., Copps, K.D., Guo, S., Li, Y., Kollipara, R., DePinho, R.A., and White, M.F. (2008). Inactivation of hepatic Foxo1 by insulin signaling is required for adaptive nutrient homeostasis and endocrine growth regulation. Cell Metab. *8*, 65–76.

Du, K., Herzig, S., Kulkarni, R.N., and Montminy, M. (2003). TRB3: a tribbles homolog that inhibits Akt/PKB activation by insulin in liver. Science *300*, 1574–1577.

Erdmann, K.S., Mao, Y., McCrea, H.J., Zoncu, R., Lee, S., Paradise, S., Modregger, J., Biemesderfer, D., Toomre, D., and De Camilli, P. (2007). A role of the Lowe syndrome protein OCRL in early steps of the endocytic pathway. Dev. Cell *13*, 377–390.

Fiory, F., Oriente, F., Miele, C., Romano, C., Trencia, A., Alberobello, A.T., Esposito, I., Valentino, R., Beguinot, F., and Formisano, P. (2004). Protein kinase C-ζ and protein kinase B regulate distinct steps of insulin endocytosis and intracellular sorting. J. Biol. Chem. *279*, 11137–11145.

He, L., Simmen, F.A., Mehendale, H.M., Ronis, M.J., and Badger, T.M. (2006). Chronic ethanol intake impairs insulin signaling in rats by disrupting Akt association with the cell membrane. Role of TRB3 in inhibition of Akt/protein kinase B activation. J. Biol. Chem. *281*, 11126–11134.

Hosch, S.E., Olefsky, J.M., and Kim, J.J. (2006). APPLied mechanics: uncovering how adiponectin modulates insulin action. Cell Metab. *4*, 5–6.

Huang, J., Imamura, T., and Olefsky, J.M. (2001). Insulin can regulate GLUT4 internalization by signaling to Rab5 and the motor protein dynein. Proc. Natl. Acad. Sci. USA *98*, 13084–13089.

Inoue, G., Cheatham, B., and Kahn, C.R. (1996). Different pathways of postreceptor desensitization following chronic insulin treatment and in cells overexpressing constitutively active insulin receptors. J. Biol. Chem. *271*, 28206–28211.

Kato, S., and Du, K. (2007). TRB3 modulates C2C12 differentiation by interfering with Akt activation. Biochem. Biophys. Res. Commun. *353*, 933–938.

Khan, M.N., Baquiran, G., Brule, C., Burgess, J., Foster, B., Bergeron, J.J., and Posner, B.I. (1989). Internalization and activation of the rat liver insulin receptor kinase in vivo. J. Biol. Chem. *264*, 12931–12940.

Koo, S.H., Satoh, H., Herzig, S., Lee, C.H., Hedrick, S., Kulkarni, R., Evans, R.M., Olefsky, J., and Montminy, M. (2004). PGC-1 promotes insulin resistance in liver through PPAR-α-dependent induction of TRB-3. Nat. Med. *10*, 530–534.

Li, J., Mao, X., Dong, L.Q., Liu, F., and Tong, L. (2007a). Crystal structures of the BAR-PH and PTB domains of human APPL1. Structure *15*, 525–533.

Li, X., Monks, B., Ge, Q., and Birnbaum, M.J. (2007b). Akt/PKB regulates hepatic metabolism by directly inhibiting PGC-1α transcription coactivator. Nature *447*, 1012–1016.

Lin, D.C., Quevedo, C., Brewer, N.E., Bell, A., Testa, J.R., Grimes, M.L., Miller, F.D., and Kaplan, D.R. (2006). APPL1 associates with TrkA and GIPC1, and is required for nerve growth factor-mediated signal transduction. Mol. Cell. Biol. *26*, 8928–8941.

Liu, J., Yao, F., Wu, R., Morgan, M., Thorburn, A., Finley, R.L., Jr., and Chen, Y.Q. (2002). Mediation of the DCC apoptotic signal by DIP13 α. J. Biol. Chem. *277*, 26281–26285.

Magnusson, I., Rothman, D.L., Katz, L.D., Shulman, R.G., and Shulman, G.I. (1992). Increased rate of gluconeogenesis in type II diabetes mellitus. A ^{13}C nuclear magnetic resonance study. J. Clin. Invest. *90*, 1323–1327.

Mao, X., Kikani, C.K., Riojas, R.A., Langlais, P., Wang, L., Ramos, F.J., Fang, Q., Christ-Roberts, C.Y., Hong, J.Y., Kim, R.Y., et al. (2006). APPL1 binds to adiponectin receptors and mediates adiponectin signalling and function. Nat. Cell Biol. *8*, 516–523.

Miaczynska, M., Christoforidis, S., Giner, A., Shevchenko, A., Uttenweiler-Joseph, S., Habermann, B., Wilm, M., Parton, R.G., and Zerial, M. (2004). APPL proteins link Rab5 to nuclear signal transduction via an endosomal compartment. Cell *116*, 445–456.

Mitsuuchi, Y., Johnson, S.W., Sonoda, G., Tanno, S., Golemis, E.A., and Testa, J.R. (1999). Identification of a chromosome 3p14.3-21.1 gene, APPL, encoding an adaptor molecule that interacts with the oncoprotein-serine/threonine kinase AKT2. Oncogene *18*, 4891–4898.

Nakae, J., Biggs, W.H., III, Kitamura, T., Cavenee, W.K., Wright, C.V., Arden, K.C., and Accili, D. (2002). Regulation of insulin action and pancreatic β-cell function by mutated alleles of the gene encoding forkhead transcription factor Foxo1. Nat. Genet. *32*, 245–253.

Nave, B.T., Haigh, R.J., Hayward, A.C., Siddle, K., and Shepherd, P.R. (1996). Compartment-specific regulation of phosphoinositide 3-kinase by platelet-derived growth factor and insulin in 3T3-L1 adipocytes. Biochem. J. *318*, 55–60.

Nechamen, C.A., Thomas, R.M., Cohen, B.D., Acevedo, G., Poulikakos, P.I., Testa, J.R., and Dias, J.A. (2004). Human follicle-stimulating hormone (FSH) receptor interacts with the adaptor protein APPL1 in HEK 293 cells: potential involvement of the PI3K pathway in FSH signaling. Biol. Reprod. *71*, 629–636.

Puigserver, P., Rhee, J., Donovan, J., Walkey, C.J., Yoon, J.C., Oriente, F., Kitamura, Y., Altomonte, J., Dong, H., Accili, D., and Spiegelman, B.M. (2003). Insulin-regulated hepatic gluconeogenesis through FOXO1-PGC-1α interaction. Nature *423*, 550–555.

Saito, T., Jones, C.C., Huang, S., Czech, M.P., and Pilch, P.F. (2007). The interaction of Akt with APPL1 is required for insulin-stimulated Glut4 translocation. J. Biol. Chem. *282*, 32280–32287.

Schenck, A., Goto-Silva, L., Collinet, C., Rhinn, M., Giner, A., Habermann, B., Brand, M., and Zerial, M. (2008). The endosomal protein Appl1 mediates Akt substrate specificity and cell survival in vertebrate development. Cell *133*, 486–497.

Su, X., Lodhi, I.J., Saltiel, A.R., and Stahl, P.D. (2006). Insulin-stimulated interaction between insulin receptor substrate 1 and p85α and activation of protein kinase B/Akt require Rab5. J. Biol. Chem. *281*, 27982–27990.

Varsano, T., Dong, M.Q., Niesman, I., Gacula, H., Lou, X., Ma, T., Testa, J.R., Yates, J.R., III, and Farquhar, M.G. (2006). GIPC is recruited by APPL to peripheral TrkA endosomes and regulates TrkA trafficking and signaling. Mol. Cell. Biol. *26*, 8942–8952.

Wang, Y., Xu, A., Knight, C., Xu, L.Y., and Cooper, G.J. (2002). Hydroxylation and glycosylation of the four conserved lysine residues in the collagenous domain of adiponectin. Potential role in the modulation of its insulin-sensitizing activity. J. Biol. Chem. *277*, 19521–19529.

Xu, A., Lam, M.C., Chan, K.W., Wang, Y., Zhang, J., Hoo, R.L., Xu, J.Y., Chen, B., Chow, W.S., Tso, A.W., and Lam, K.S. (2005). Angiopoietin-like protein 4 decreases blood glucose and improves glucose tolerance but induces hyperlipidemia and hepatic steatosis in mice. Proc. Natl. Acad. Sci. USA *102*, 6086–6091.

Yang, L., Lin, H.K., Altuwaijri, S., Xie, S., Wang, L., and Chang, C. (2003). APPL suppresses androgen receptor transactivation via potentiating Akt activity. J. Biol. Chem. *278*, 16820–16827.

Zhou, G., Myers, R., Li, Y., Chen, Y., Shen, X., Fenyk-Melody, J., Wu, M., Ventre, J., Doebber, T., Fujii, N., et al. (2001). Role of AMP-activated protein kinase in mechanism of metformin action. J. Clin. Invest. *108*, 1167–1174.